

New Measurement of Time-Dependent CP -Violating Asymmetry in $B^0 \rightarrow K_S^0 \pi^0 \gamma$ Decay

Y. Ushiroda,⁷ K. Sumisawa,^{28,7} M. Hazumi,⁷ K. Abe,⁷ K. Abe,³⁸ I. Adachi,⁷ H. Aihara,⁴⁰ Y. Asano,⁴⁴
V. Aulchenko,¹ T. Aushev,¹⁰ A. M. Bakich,³⁵ A. Bay,¹⁵ I. Bedny,¹ U. Bitenc,¹¹ I. Bizjak,¹¹ S. Blyth,²³ A. Bondar,¹
A. Bozek,²⁴ M. Bračko,^{7,17,11} J. Brodzicka,²⁴ T. E. Browder,⁶ M.-C. Chang,²³ P. Chang,²³ Y. Chao,²³ A. Chen,²¹
W. T. Chen,²¹ B. G. Cheon,³ S.-K. Choi,⁵ Y. Choi,³⁴ A. Chuvikov,⁴⁷ S. Cole,³⁵ J. Dalseno,¹⁸ M. Danilov,¹⁰
M. Dash,⁴⁵ J. Dragic,¹⁸ S. Eidelman,¹ F. Fang,⁶ S. Fratina,¹¹ N. Gabyshev,¹ T. Gershon,⁷ G. Gokhroo,³⁶
A. Gorišek,¹¹ J. Haba,⁷ K. Hara,⁷ N. C. Hastings,⁴⁰ K. Hayasaka,¹⁹ H. Hayashii,²⁰ T. Higuchi,⁷ L. Hinz,¹⁵
T. Hokuue,¹⁹ Y. Hoshi,³⁸ S. Hou,²¹ W.-S. Hou,²³ Y. B. Hsiung,²³ T. Iijima,¹⁹ A. Imoto,²⁰ K. Inami,¹⁹
A. Ishikawa,⁷ H. Ishino,⁴¹ R. Itoh,⁷ M. Iwasaki,⁴⁰ Y. Iwasaki,⁷ J. H. Kang,⁴⁶ J. S. Kang,¹³ P. Kapusta,²⁴
N. Katayama,⁷ H. Kawai,² T. Kawasaki,²⁶ H. R. Khan,⁴¹ H. Kichimi,⁷ H. J. Kim,¹⁴ S. M. Kim,³⁴ K. Kinoshita,⁴
P. Križan,^{16,11} P. Krokovny,¹ S. Kumar,²⁹ C. C. Kuo,²¹ A. Kusaka,⁴⁰ A. Kuzmin,¹ Y.-J. Kwon,⁴⁶
G. Leder,⁹ T. Lesiak,²⁴ J. Li,³² A. Limosani,¹⁸ S.-W. Lin,²³ D. Liventsev,¹⁰ F. Mandl,⁹ T. Matsumoto,⁴²
Y. Mikami,³⁹ W. Mitaroff,⁹ K. Miyabayashi,²⁰ H. Miyake,²⁸ H. Miyata,²⁶ D. Mohapatra,⁴⁵ G. R. Moloney,¹⁸
T. Nagamine,³⁹ E. Nakano,²⁷ M. Nakao,⁷ S. Nishida,⁷ O. Nitoh,⁴³ T. Nozaki,⁷ S. Ogawa,³⁷ T. Ohshima,¹⁹
T. Okabe,¹⁹ S. Okuno,¹² S. L. Olsen,⁶ W. Ostrowicz,²⁴ H. Ozaki,⁷ P. Pakhlov,¹⁰ H. Palka,²⁴ C. W. Park,³⁴
N. Parslow,³⁵ L. S. Peak,³⁵ R. Pestotnik,¹¹ L. E. Piiilonen,⁴⁵ H. Sagawa,⁷ Y. Sakai,⁷ N. Sato,¹⁹ T. Schietinger,¹⁵
O. Schneider,¹⁵ A. J. Schwartz,⁴ K. Senyo,¹⁹ M. E. Sevier,¹⁸ T. Shibata,²⁶ H. Shibuya,³⁷ J. B. Singh,²⁹
A. Somov,⁴ N. Soni,²⁹ R. Stamen,⁷ S. Stanič,^{44,*} M. Starič,¹¹ T. Sumiyoshi,⁴² S. Suzuki,³¹ O. Tajima,⁷
F. Takasaki,⁷ K. Tamai,⁷ N. Tamura,²⁶ M. Tanaka,⁷ Y. Teramoto,²⁷ X. C. Tian,³⁰ K. Trabelsi,⁶ T. Tsuboyama,⁷
T. Tsukamoto,⁷ S. Uehara,⁷ T. Uglov,¹⁰ S. Uno,⁷ P. Urquijo,¹⁸ G. Varner,⁶ K. E. Varvell,³⁵ S. Villa,¹⁵
C. C. Wang,²³ C. H. Wang,²² M. Watanabe,²⁶ Y. Watanabe,⁴¹ Q. L. Xie,⁸ A. Yamaguchi,³⁹ Y. Yamashita,²⁵
M. Yamauchi,⁷ Heyoung Yang,³³ J. Ying,³⁰ J. Zhang,⁷ L. M. Zhang,³² Z. P. Zhang,³² and D. Žontar^{16,11}

(The Belle Collaboration)

¹*Budker Institute of Nuclear Physics, Novosibirsk*

²*Chiba University, Chiba*

³*Chonnam National University, Kwangju*

⁴*University of Cincinnati, Cincinnati, Ohio 45221*

⁵*Gyeongsang National University, Chinju*

⁶*University of Hawaii, Honolulu, Hawaii 96822*

⁷*High Energy Accelerator Research Organization (KEK), Tsukuba*

⁸*Institute of High Energy Physics, Chinese Academy of Sciences, Beijing*

⁹*Institute of High Energy Physics, Vienna*

¹⁰*Institute for Theoretical and Experimental Physics, Moscow*

¹¹*J. Stefan Institute, Ljubljana*

¹²*Kanagawa University, Yokohama*

¹³*Korea University, Seoul*

¹⁴*Kyungpook National University, Taegu*

¹⁵*Swiss Federal Institute of Technology of Lausanne, EPFL, Lausanne*

¹⁶*University of Ljubljana, Ljubljana*

¹⁷*University of Maribor, Maribor*

¹⁸*University of Melbourne, Victoria*

¹⁹*Nagoya University, Nagoya*

²⁰*Nara Women's University, Nara*

²¹*National Central University, Chung-li*

²²*National United University, Miao Li*

²³*Department of Physics, National Taiwan University, Taipei*

²⁴*H. Niewodniczanski Institute of Nuclear Physics, Krakow*

²⁵*Nihon Dental College, Niigata*

²⁶*Niigata University, Niigata*

²⁷*Osaka City University, Osaka*

²⁸*Osaka University, Osaka*

²⁹*Panjab University, Chandigarh*

³⁰*Peking University, Beijing*

- ³¹Saga University, Saga
³²University of Science and Technology of China, Hefei
³³Seoul National University, Seoul
³⁴Sungkyunkwan University, Suwon
³⁵University of Sydney, Sydney NSW
³⁶Tata Institute of Fundamental Research, Bombay
³⁷Toho University, Funabashi
³⁸Tohoku Gakuin University, Tagajo
³⁹Tohoku University, Sendai
⁴⁰Department of Physics, University of Tokyo, Tokyo
⁴¹Tokyo Institute of Technology, Tokyo
⁴²Tokyo Metropolitan University, Tokyo
⁴³Tokyo University of Agriculture and Technology, Tokyo
⁴⁴University of Tsukuba, Tsukuba
⁴⁵Virginia Polytechnic Institute and State University, Blacksburg, Virginia 24061
⁴⁶Yonsei University, Seoul
⁴⁷Princeton University, Princeton, New Jersey 08545
(Dated: December 2, 2024)

We present a new measurement of CP -violation parameters in $B^0 \rightarrow K_S^0 \pi^0 \gamma$ decay based on a sample of $275 \times 10^6 B\bar{B}$ pairs collected at the $\Upsilon(4S)$ resonance with the Belle detector at the KEKB energy-asymmetric e^+e^- collider. One of the B mesons is fully reconstructed in the $B^0 \rightarrow K_S^0 \pi^0 \gamma$ decay. The flavor of the accompanying B meson is identified from its decay products. CP -violation parameters are obtained from the asymmetry in the distribution of the proper-time intervals between the two B decays. We obtain $\mathcal{S}_{K_S^0 \pi^0 \gamma} = -0.58_{-0.38}^{+0.46}(\text{stat}) \pm 0.11(\text{syst})$ and $\mathcal{A}_{K_S^0 \pi^0 \gamma} = +0.03 \pm 0.34(\text{stat}) \pm 0.11(\text{syst})$, for the $K_S^0 \pi^0$ invariant mass covering the full range up to $1.8 \text{ GeV}/c^2$. We also measure the CP -violation parameters for the case $B^0 \rightarrow K^{*0}(\rightarrow K_S^0 \pi^0) \gamma$ and obtain $\mathcal{S}_{K^{*0} \gamma} = -0.79_{-0.50}^{+0.63}(\text{stat}) \pm 0.10(\text{syst})$ for $\mathcal{A}_{K^{*0} \gamma}$ fixed at 0.

PACS numbers: 11.30.Er, 12.15.Hh, 13.25.Hw

In the Standard Model (SM), CP violation arises from an irreducible phase, the Kobayashi-Maskawa (KM) phase [1], in the weak-interaction quark-mixing matrix. In particular, the SM predicts CP asymmetries in the time-dependent rates for B^0 and \bar{B}^0 decays to a common CP eigenstate f_{CP} [2]. In the decay chain $\Upsilon(4S) \rightarrow B^0 \bar{B}^0 \rightarrow f_{CP} f_{\text{tag}}$, where one of the B mesons decays at time t_{CP} to a final state f_{CP} and the other decays at time t_{tag} to a final state f_{tag} that distinguishes between B^0 and \bar{B}^0 , the decay rate has a time dependence given by

$$\mathcal{P}(\Delta t) = \frac{e^{-|\Delta t|/\tau_{B^0}}}{4\tau_{B^0}} \left\{ 1 + q \left[\mathcal{S} \sin(\Delta m_d \Delta t) + \mathcal{A} \cos(\Delta m_d \Delta t) \right] \right\}. \quad (1)$$

Here \mathcal{S} and \mathcal{A} are CP -violation parameters, τ_{B^0} is the B^0 lifetime, Δm_d is the mass difference between the two B^0 mass eigenstates, Δt is the time difference $t_{CP} - t_{\text{tag}}$, and the b -flavor charge $q = +1$ (-1) when the tagging B meson is a B^0 (\bar{B}^0).

The phenomena of time-dependent CP violation in decays through radiative penguin processes such as $b \rightarrow s \gamma$ are sensitive to physics beyond the SM [3, 4]. Within the SM, the photon emitted from a B^0 (\bar{B}^0) meson is dominantly right-handed (left-handed). Therefore the polarization of the photon carries information on the original

b -flavor and the decay is, thus, almost flavor-specific. As a result, the SM predicts a small asymmetry [3] and any significant deviation from this expectation would be a manifestation of new physics. Recently it was pointed out that in decays of the type $B^0 \rightarrow P^0 Q^0 \gamma$, where P^0 and Q^0 represent any CP eigenstate spin-0 neutral particles (e.g. $P^0 = K_S^0$ and $Q^0 = \pi^0$), possible new physics effects on the mixing-induced CP violation do not depend on the resonant structure of the $P^0 Q^0$ system [4]. In this Letter, we describe two measurements of CP asymmetries: one with a $K_S^0 \pi^0$ mass range restricted around the K^{*0} [5] mass, and the other with an extended $K_S^0 \pi^0$ mass range based on the new proposal. Whenever necessary, we distinguish these two by referring to them as $K^{*0} \gamma$ and $K_S^0 \pi^0 \gamma$, respectively; otherwise the analysis procedure is common to both measurements since it was first optimized for the $K^{*0} \gamma$ and was extended for the $K_S^0 \pi^0 \gamma$ later.

At the KEKB energy-asymmetric e^+e^- (3.5 on 8.0 GeV) collider [6], the $\Upsilon(4S)$ is produced with a Lorentz boost of $\beta\gamma = 0.425$ along the z axis defined as antiparallel to the e^+ beam direction. Since the B^0 and \bar{B}^0 mesons are approximately at rest in the $\Upsilon(4S)$ center-of-mass system (cms), Δt can be determined from the displacement in z between the f_{CP} and f_{tag} decay vertices: $\Delta t \simeq (z_{CP} - z_{\text{tag}})/(\beta\gamma c) \equiv \Delta z/(\beta\gamma c)$.

The Belle detector [7] is a large-solid-angle magnetic spectrometer that consists of a silicon vertex detector

(SVD), a 50-layer central drift chamber, an array of aerogel threshold Cherenkov counters, a barrel-like arrangement of time-of-flight scintillation counters, an electromagnetic calorimeter (ECL) and an iron flux-return instrumented to detect K_L^0 mesons and to identify muons. A 2.0 cm radius beampipe and a 3-layer SVD (SVD1) were used for a 140 fb^{-1} data sample containing 152×10^6 $B\bar{B}$ pairs, while a 1.5 cm radius beampipe, a 4-layer silicon detector (SVD2) [8] and a small-cell inner drift chamber were used for an additional 113 fb^{-1} data sample that contains 123×10^6 $B\bar{B}$ pairs for a total of 275×10^6 $B\bar{B}$ pairs.

For high energy prompt photons, we select an isolated cluster in the ECL that has no corresponding charged track, and has the largest energy in the cms. We require the shower shape to be consistent with that of a photon. In order to reduce the background from π^0 or η , we exclude photons compatible with $\pi^0 \rightarrow \gamma\gamma$ or $\eta \rightarrow \gamma\gamma$ decays; we reject photon pairs that satisfy $\mathcal{L}_{\pi^0} \geq 0.18$ or $\mathcal{L}_{\eta} \geq 0.18$, where $\mathcal{L}_{\pi^0(\eta)}$ is a π^0 (η) likelihood described in detail elsewhere [9]. The polar angle of the photon direction in the laboratory frame is restricted to the barrel region of the ECL ($33^\circ < \theta_\gamma < 128^\circ$), but is extended to the end-cap regions ($17^\circ < \theta_\gamma < 150^\circ$) for the second data sample due to the reduced material in front of the ECL.

Neutral kaons (K_S^0) are reconstructed from two oppositely charged pions that have an invariant mass within $\pm 6 \text{ MeV}/c^2$ (2σ) of the K_S^0 nominal mass. The $\pi^+\pi^-$ vertex is required to be displaced from the interaction point (IP) in the direction of the pion pair momentum [10]. Neutral pions (π^0) are formed from two photons with the invariant mass within $\pm 16 \text{ MeV}/c^2$ (3σ) of the π^0 mass. The photon momenta are then recalculated with a π^0 mass constraint and we require the momentum of π^0 candidates in the laboratory frame to be greater than $0.3 \text{ GeV}/c$. The $K_S^0\pi^0$ invariant mass, $M_{K_S^0\pi^0}$, is required to be less than $1.8 \text{ GeV}/c^2$.

B^0 mesons are reconstructed by combining K_S^0 , π^0 and γ candidates. We form two kinematic variables: the energy difference $\Delta E \equiv E_B^{\text{cms}} - E_{\text{beam}}^{\text{cms}}$ and the beam-energy constrained mass $M_{\text{bc}} \equiv \sqrt{(E_{\text{beam}}^{\text{cms}})^2 - (p_B^{\text{cms}})^2}$, where $E_{\text{beam}}^{\text{cms}}$ is the beam energy, E_B^{cms} and p_B^{cms} are the energy and the momentum of the candidate in the cms. Candidates are accepted if they have $M_{\text{bc}} > 5.2 \text{ GeV}/c^2$ and $|\Delta E| < 0.5 \text{ GeV}$.

We reconstruct $B^+ \rightarrow K_S^0\pi^+\gamma$ candidates in a similar way as the $B^0 \rightarrow K_S^0\pi^0\gamma$ decay in order to reduce the cross-feed background from $B^+ \rightarrow K_S^0\pi^+\gamma$ in $B^0 \rightarrow K_S^0\pi^0\gamma$. The $B^+ \rightarrow K_S^0\pi^+\gamma$ events are also used for various cross-checks. For a π^+ candidate, we require that the track originates from the IP and that the transverse momentum is greater than $0.1 \text{ GeV}/c$. We also require that the π^+ candidate cannot be identified as any other particle species (K^+ , p^+ , e^+ , and μ^+).

Candidate $B^+ \rightarrow K_S^0\pi^+\gamma$ and $B^0 \rightarrow K_S^0\pi^0\gamma$ decays are

selected simultaneously; we allow only one candidate for each event. The best candidate selection is based on the event likelihood ratio $\mathcal{R}_{s/b}$ that is obtained by combining a Fisher discriminant \mathcal{F} [11], which uses the extended modified Fox-Wolfram moments [12] as discriminating variables, and $\cos\theta_H$ defined as the angle between the B meson momentum and the daughter K_S^0 momentum in the rest frame of the $K_S^0\pi$ system. We select the candidate that has the largest $\mathcal{R}_{s/b}$. For the exclusive $B^0 \rightarrow K^{*0}\gamma$ study, we further require $0.8 \text{ GeV}/c^2 < M_{K_S^0\pi^0} < 1.0 \text{ GeV}/c^2$ after the best candidate selection. The signal region is defined as $-0.2 \text{ GeV} < \Delta E < 0.1 \text{ GeV}$ and $5.27 \text{ GeV}/c^2 < M_{\text{bc}} < 5.29 \text{ GeV}/c^2$.

We use events outside the signal region as well as large Monte Carlo (MC) samples to study the background components. The dominant background is from continuum light quark pair production ($e^+e^- \rightarrow q\bar{q}$ with $q = u, d, s, c$), which we refer to as $q\bar{q}$ hereafter. We require $\mathcal{R}_{s/b} > 0.5$ to reduce the $q\bar{q}$ background; after applying all other selection criteria, this rejects 79% of the $q\bar{q}$ background while retaining 88% of the signal. Background contributions from B decays, which are considerably smaller than $q\bar{q}$, are dominated by cross-feed from other radiative B decays including $B^+ \rightarrow K_S^0\pi^+\gamma$.

The b -flavor of the accompanying B meson is identified from inclusive properties of particles that are not associated with the reconstructed signal decay. The algorithm for flavor tagging is described in detail elsewhere [13]. We use two parameters, q defined in Eq. (1) and r , to represent the tagging information. The parameter r is an event-by-event flavor-tagging dilution factor that ranges from 0 to 1; $r = 0$ when there is no flavor discrimination and $r = 1$ implies unambiguous flavor assignment. It is determined by using MC data and is only used to sort data into six r intervals. The wrong tag fraction w and the difference Δw in w for the B^0 and \bar{B}^0 decays are determined for each of the six r intervals from data [10].

The vertex position of the signal-side decay is reconstructed from the K_S^0 trajectory with a constraint on the IP; the IP profile ($\sigma_x \simeq 100 \mu\text{m}$, $\sigma_y \simeq 5 \mu\text{m}$, $\sigma_z \simeq 3 \text{ mm}$) is convolved with the finite B flight length in the plane perpendicular to the z axis. Both pions from the K_S^0 decay are required to have enough hits in the SVD in order to reconstruct the K_S^0 trajectory with high resolution. The reconstruction efficiency depends not only on the K_S^0 momentum but also on the SVD geometry. The efficiency with SVD2 (55%) is higher than with SVD1 (41%) because of the larger detection volume. The other (tag-side) B vertex determination is the same as that for the $B^0 \rightarrow \phi K_S^0$ analysis [10].

Figure 1 shows the M_{bc} (ΔE) distribution for the reconstructed $K_S^0\pi^0\gamma$ candidates within the ΔE (M_{bc}) signal region after flavor tagging and vertex reconstruction. The signal yield is determined from an unbinned two-dimensional maximum-likelihood fit to the ΔE - M_{bc} distribution. The fit region for the $B^0 \rightarrow K^{*0}\gamma$ analysis

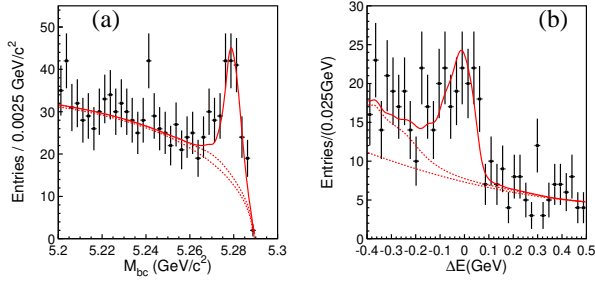


FIG. 1: (a) M_{bc} distributions within the ΔE signal region and (b) ΔE distributions within the M_{bc} signal region for $B^0 \rightarrow K_S^0 \pi^0 \gamma$. Solid curves show the fit to signal plus background distributions. Lower (upper) dashed curves show the background contributions from $q\bar{q}$ ($q\bar{q}$ and B decays).

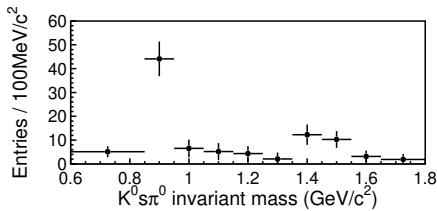


FIG. 2: $M_{K_S^0 \pi^0}$ distribution of the $B^0 \rightarrow K_S^0 \pi^0 \gamma$ signal yield obtained from the fit to the ΔE - M_{bc} distribution. Background shape parameters are fixed at the values obtained with the whole $M_{K_S^0 \pi^0}$ region.

is $5.20 \text{ GeV}/c^2 < M_{bc} < 5.29 \text{ GeV}/c^2$ and $-0.5 \text{ GeV} < \Delta E < 0.5 \text{ GeV}$. For the $B^0 \rightarrow K_S^0 \pi^0 \gamma$ analysis, the ΔE fit region is narrowed to $-0.4 \text{ GeV} < \Delta E < 0.5 \text{ GeV}$ in order to avoid other B background events that populate the low ΔE region. The signal distribution is represented by a smoothed histogram obtained from MC simulation that accounts for a small correlation between M_{bc} and ΔE . The background from B decays is also modeled with a smoothed histogram obtained from MC events. For the $q\bar{q}$ background, we use the ARGUS parameterization [14] for M_{bc} and a second-order polynomial for ΔE . Normalizations of the signal and background distributions and the $q\bar{q}$ background shape are the five free parameters in the fit. We observe 501 (215) $K_S^0 \pi^0 \gamma$ ($K^{*0} \gamma$) candidates in the signal box, which decrease to 227 (92) after the flavor tagging and the B vertex reconstruction, and obtain 105 ± 14 (57 ± 9) signal events by the fit. Figure 2 shows the signal yields in different $M_{K_S^0 \pi^0}$ regions. For each bin, a fit to the ΔE - M_{bc} distribution is performed, and the obtained signal yield is plotted.

We determine \mathcal{S} and \mathcal{A} from an unbinned maximum-likelihood fit to the observed Δt distribution. The probability density function (PDF) expected for the signal distribution, $\mathcal{P}_{\text{sig}}(\Delta t; \mathcal{S}, \mathcal{A}, q, w, \Delta w)$, is given by the time dependent decay rate [Eq. (1)] modified to incorporate the effect of incorrect flavor assignment. The distribu-

tion is convolved with the proper-time interval resolution function R_{sig} , which takes into account the finite vertex resolution. The parametrization of R_{sig} is the same as that used for the $B^0 \rightarrow K_S^0 \pi^0$ decay [10]. R_{sig} is first derived from flavor-specific B decays [15] and modified by additional parameters which rescale vertex errors to account for the fact that there is no track directly originating from the IP.

For each event, the following likelihood function is evaluated:

$$\begin{aligned}
 P_i = & (1 - f_{\text{ol}}) \int_{-\infty}^{+\infty} \left[f_{\text{sig}} \mathcal{P}_{\text{sig}}(\Delta t') R_{\text{sig}}(\Delta t_i - \Delta t') \right. \\
 & + (1 - f_{\text{sig}}) \mathcal{P}_{\text{bkg}}(\Delta t') R_{\text{bkg}}(\Delta t_i - \Delta t') \left. \right] d(\Delta t') \\
 & + f_{\text{ol}} P_{\text{ol}}(\Delta t_i),
 \end{aligned} \tag{2}$$

where P_{ol} is a Gaussian function that represents a small outlier component with fraction f_{ol} . The signal probability f_{sig} is calculated on an event-by-event basis from the function which we obtained as the result of the two-dimensional ΔE - M_{bc} fit for the signal yield extraction. A PDF for background events, \mathcal{P}_{bkg} , is modeled as a sum of exponential and prompt components, and is convolved with a sum of two Gaussians which represent the resolution function R_{bkg} for the background. All parameters in \mathcal{P}_{bkg} and R_{bkg} are determined by a fit to the Δt distribution of a background-enhanced control sample, i.e. events outside of the ΔE - M_{bc} signal region. We fix τ_{B^0} and Δm_d at their world-average values [16].

The only free parameters in the final fit for the $B^0 \rightarrow K_S^0 \pi^0 \gamma$ decay are $\mathcal{S}_{K_S^0 \pi^0 \gamma}$ and $\mathcal{A}_{K_S^0 \pi^0 \gamma}$, which are determined by maximizing the likelihood function $L = \prod_i P_i(\Delta t_i; \mathcal{S}, \mathcal{A})$ where the product is over all events. For the $B^0 \rightarrow K^{*0} \gamma$ decay, we fix $\mathcal{A}_{K^{*0} \gamma}$ at zero and perform a single parameter fit for $\mathcal{S}_{K^{*0} \gamma}$. This is based on the previous measurement [17] of the partial rate asymmetry in $B \rightarrow K^* \gamma$ decays, which yielded $\mathcal{A}_{K^{*0} \gamma}$ consistent with zero. The error of the previous measurement of $\mathcal{A}_{K^{*0} \gamma}$ is included in the systematic error of $\mathcal{S}_{K^{*0} \gamma}$. We obtain

$$\begin{aligned}
 \mathcal{S}_{K^{*0} \gamma} &= -0.79_{-0.50}^{+0.63}(\text{stat}) \pm 0.10(\text{syst}), \\
 \mathcal{S}_{K_S^0 \pi^0 \gamma} &= -0.58_{-0.38}^{+0.46}(\text{stat}) \pm 0.11(\text{syst}), \\
 \mathcal{A}_{K_S^0 \pi^0 \gamma} &= +0.03 \pm 0.34(\text{stat}) \pm 0.11(\text{syst}).
 \end{aligned}$$

We define the raw asymmetry in each Δt bin by $(N_{q=+1} - N_{q=-1}) / (N_{q=+1} + N_{q=-1})$, where $N_{q=+1(-1)}$ is the number of observed candidates with $q = +1(-1)$. Figure 3 shows the raw asymmetries for the $K_S^0 \pi^0 \gamma$ and $K^{*0} \gamma$ decays in two regions of the flavor-tagging parameter r . Note that these are simple projections onto the Δt axis, and do not reflect other event-by-event information (such as the signal fraction, the wrong tag fraction and the vertex resolution), which is in fact used in the unbinned maximum-likelihood fit for \mathcal{S} and \mathcal{A} .

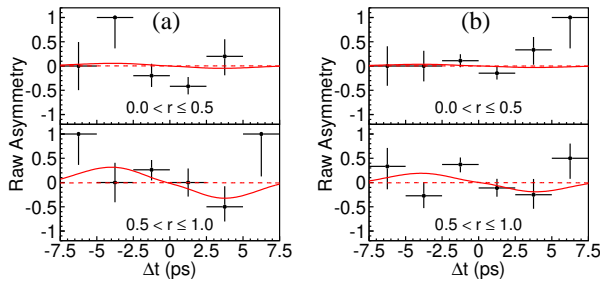


FIG. 3: Asymmetry in each Δt bin with $0 < r \leq 0.5$ (top) and with $0.5 < r \leq 1.0$ (bottom) for (a) $B^0 \rightarrow K^{*0}\gamma$ and for (b) $B^0 \rightarrow K_S^0\pi^0\gamma$. Solid curves show the results of the unbinned maximum-likelihood fits. The dashed curves show the null asymmetry case ($\mathcal{S} = \mathcal{A} = 0$). The dilution of a possible asymmetry is smaller for the $0.5 < r \leq 1.0$ subsample, because of the lower probability of incorrect flavor assignment.

Primary sources of the systematic error are (1) uncertainties in the resolution function (± 0.05 for $\mathcal{S}_{K_S^0\pi^0\gamma}$, ± 0.04 for $\mathcal{A}_{K_S^0\pi^0\gamma}$ and ± 0.05 for $\mathcal{S}_{K^{*0}\gamma}$), (2) uncertainties in the vertex reconstruction (± 0.05 for $\mathcal{S}_{K_S^0\pi^0\gamma}$, ± 0.06 for $\mathcal{A}_{K_S^0\pi^0\gamma}$ and ± 0.06 for $\mathcal{S}_{K^{*0}\gamma}$), (3) uncertainties in the background fraction (± 0.06 for $\mathcal{S}_{K_S^0\pi^0\gamma}$, ± 0.04 for $\mathcal{A}_{K_S^0\pi^0\gamma}$ and ± 0.02 for $\mathcal{S}_{K^{*0}\gamma}$), and (4) uncertainties in the background Δt distribution (± 0.05 for $\mathcal{S}_{K_S^0\pi^0\gamma}$, ± 0.04 for $\mathcal{A}_{K_S^0\pi^0\gamma}$ and ± 0.02 for $\mathcal{S}_{K^{*0}\gamma}$). Effects of tag-side interference [18] contribute ± 0.01 for $\mathcal{S}_{K_S^0\pi^0\gamma}$, ± 0.06 for $\mathcal{A}_{K_S^0\pi^0\gamma}$ and ± 0.01 for $\mathcal{S}_{K^{*0}\gamma}$. Also included are effects from uncertainties in the wrong tag fraction and physics parameters (Δm_d , τ_{B^0} and $\mathcal{A}_{K^{*0}\gamma}$). A possible bias in the fit is estimated by using MC data. The total systematic error is obtained by adding these contributions in quadrature.

Various cross-checks of the measurement are performed. We apply the same fit procedure to the $B^0 \rightarrow J/\psi K_S^0$ sample without using J/ψ daughter tracks for the vertex reconstruction. We obtain $\mathcal{S}_{J/\psi K_S^0} = +0.68 \pm 0.10(\text{stat})$ and $\mathcal{A}_{J/\psi K_S^0} = +0.02 \pm 0.04(\text{stat})$, which are in good agreement with the world average values [16]. We perform a fit to $B^+ \rightarrow K_S^0\pi^+\gamma$ ($B^+ \rightarrow K^{*+}\gamma \rightarrow K_S^0\pi^+\gamma$), which is a good control sample of the $B^0 \rightarrow K_S^0\pi^0\gamma$ ($B^0 \rightarrow K^{*0}\gamma \rightarrow K_S^0\pi^0\gamma$) decay, without using the primary π^+ for the vertex reconstruction. The result is consistent with no CP asymmetry, as expected. Lifetime measurements are also performed for these modes, and values consistent with the world-average are obtained. Ensemble tests are carried out with MC pseudo-experiments; we find that the statistical errors obtained in our measurements are all within the expectations from the ensemble tests. A fit to the $B^0 \rightarrow K_S^0\pi^0\gamma$ subsample that excludes the K^{*0} mass region yields $\mathcal{S} = -0.39_{-0.52}^{+0.63}(\text{stat})$ and $\mathcal{A} = +0.10 \pm 0.51(\text{stat})$. The result is consistent with the results for $B^0 \rightarrow K^{*0}\gamma$ and for the

full $B^0 \rightarrow K_S^0\pi^0\gamma$ sample.

In summary, we have performed a new measurement of the time-dependent CP asymmetry in the decay $B^0 \rightarrow K_S^0\pi^0\gamma$ based on a sample of 275×10^6 $B\bar{B}$ pairs. Two regions of the $K_S^0\pi^0$ invariant mass are used: between $0.8 \text{ GeV}/c^2$ and $1.0 \text{ GeV}/c^2$ for the K^{*0} resonance, and the full region up to $1.8 \text{ GeV}/c^2$ including other resonances and non-resonant contributions. We obtain CP -violation parameters in the $B^0 \rightarrow K_S^0\pi^0\gamma$ decay $\mathcal{S}_{K_S^0\pi^0\gamma} = -0.58_{-0.38}^{+0.46}(\text{stat}) \pm 0.11(\text{syst})$ and $\mathcal{A}_{K_S^0\pi^0\gamma} = +0.03 \pm 0.34(\text{stat}) \pm 0.11(\text{syst})$, and in $B^0 \rightarrow K^{*0}(\rightarrow K_S^0\pi^0)\gamma$ decay $\mathcal{S}_{K^{*0}\gamma} = -0.79_{-0.50}^{+0.63}(\text{stat}) \pm 0.10(\text{syst})$ with $\mathcal{A}_{K^{*0}\gamma}$ fixed at zero. The value of $\mathcal{S}_{K^{*0}\gamma}$ is consistent with the measurement by *BABAR* [19]. CP -violation parameters in the three-body $B^0 \rightarrow K_S^0\pi^0\gamma$ decay are measured for the first time. The two results are consistent with each other and with no CP asymmetry, while the statistical error is considerably reduced by the inclusion of these additional events in the $B^0 \rightarrow K_S^0\pi^0\gamma$ analysis.

We thank the KEKB group for the excellent operation of the accelerator, the KEK cryogenics group for the efficient operation of the solenoid, and the KEK computer group and the NII for valuable computing and SuperSINET network support. We acknowledge support from MEXT and JSPS (Japan); ARC and DEST (Australia); NSFC (contract No. 10175071, China); DST (India); the BK21 program of MOEHRD and the CHEP SRC program of KOSEF (Korea); KBN (contract No. 2P03B 01324, Poland); MIST (Russia); MHEST (Slovenia); SNSF (Switzerland); NSC and MOE (Taiwan); and DOE (USA).

* on leave from Nova Gorica Polytechnic, Nova Gorica

- [1] M. Kobayashi and T. Maskawa, *Prog. Theor. Phys.* **49**, 652 (1973).
- [2] A. B. Carter and A. I. Sanda, *Phys. Rev. D* **23**, 1567 (1981); I. I. Bigi and A. I. Sanda, *Nucl. Phys.* **B193**, 85 (1981).
- [3] S is suppressed by a factor of $-2(m_s/m_b)$, according to D. Atwood, M. Gronau and A. Soni, *Phys. Rev. Lett.* **79**, 185 (1997). $S \sim 0.1$ is allowed within the SM according to B. Grinstein, Y. Grossman, Z. Ligeti and D. Pirjol, *Phys. Rev. D* **71**, 011504 (2005).
- [4] D. Atwood, T. Gershon, M. Hazumi and A. Soni, *hep-ph/0410036*.
- [5] Throughout this paper, K^* denotes $K^*(892)$. The inclusion of the charge conjugate decay mode is implied.
- [6] S. Kurokawa and E. Kikutani *et al.*, *Nucl. Instr. and Meth. A* **499**, 1 (2003).
- [7] Belle Collaboration, A. Abashian *et al.*, *Nucl. Instr. and Meth. A* **479**, 117 (2002).
- [8] Y. Ushiroda (Belle SVD2 Group), *Nucl. Instr. and Meth. A* **511**, 6 (2003).
- [9] Belle Collaboration, P. Koppenburg *et al.*, *Phys. Rev. Lett.* **93**, 061803 (2004).
- [10] Belle Collaboration, K. Abe *et al.*, *hep-ex/0409049*.

- [11] R. A. Fisher, *Annals Eugen.* **7**, 179 (1936).
- [12] Belle Collaboration, K. Abe *et al.*, *Phys. Rev. Lett.* **91**, 261801 (2003).
- [13] H. Kakuno, K. Hara *et al.*, *Nucl. Instr. and Meth. A* **533**, 516 (2004).
- [14] ARGUS Collaboration, H. Albrecht *et al.*, *Phys. Lett. B* **241**, 278 (1990).
- [15] Belle Collaboration, K. Abe *et al.*, hep-ex/0408111.
- [16] S. Eidelman *et al.*, *Phys. Lett. B* **592**, 1 (2004).
- [17] Belle Collaboration, M. Nakao *et al.*, *Phys. Rev. D* **69**, 112001 (2004).
- [18] O. Long, M. Baak, R. N. Cahn and D. Kirkby, *Phys. Rev. D* **68**, 034010 (2003).
- [19] *BABAR* Collaboration, B. Aubert *et al.*, *Phys. Rev. Lett.* **93**, 201801 (2004).